*Vladimir Milovanović*
*Miroslav Živković*
*Gordana Jovičić*
*Jelena Živković*
*Dražan Kozak*

# THE INFLUENCE OF WAGON STRUCTURE PART SHAPE OPTIMIZATION ON ULTIMATE FATIGUE STRENGTH

**Summary**

This study investigates how shape optimisation affects the ultimate fatigue strength of a mechanical part. The mechanical part chosen for this investigation is an axle guard of running gear elements of the Hccrrs 2x2 axle car-carrying wagon. The static and fatigue strength analysis procedure according to the UIC 517 standard and numerical methods have been applied. Material properties were determined experimentally and the necessary numerical calculations were performed by using the finite element method. The observed axle guard is exposed to low cycle fatigue. $\varepsilon - N$ curves and material properties of the S355J2+N steel grade are obtained by combining theoretical formulae and a mathematical function. According to the obtained experimental and numerical results the number of cycles until failure for both shapes of axle guards is obtained.

*Key words:* *fatigue strength, $\varepsilon - N$ method, finite element analysis, shape optimization*

## 1. Introduction

A significant number of papers have been devoted to finding a combined methodology for fatigue strength estimation of vital structural components [1, 2, 3]. This paper presents an application of a developed methodology based on the numerical, theoretical, and experimental techniques of fatigue mechanics. The fatigue strength estimation process involves several stages: experimental definition of fatigue parameters, shape optimization, defining the numerical model, numerical calculation of strength according to corresponding standards and estimation of fatigue strength by using experimental and numerical results.

In the theory of optimal design, the design parameters (geometry) that define extreme properties (minimum-maximum) of observed machines are determined by optimization. Optimization is an applied scientific discipline that consists of mathematical programming methods, variational calculation, theory of optimal control methods and theoretical mechanics. Optimization defines the required technical characteristics of structures. In the mathematical sense, optimization is a process of finding conditions that give extreme values of the objective function.

During the design process, the main goal of each designer is to create a structure with optimal strength, minimal weight and at minimal cost. Nowadays with the progress of computer technology, designers have an opportunity to optimize each component of the structure during the design process by using the Finite Element Method (FEM).

Optimization represents a process of finding the most favourable structure solution for the set conditions. There are two types of structural optimization (Fig. 1):

1. parametric optimization and
2. shape optimization.
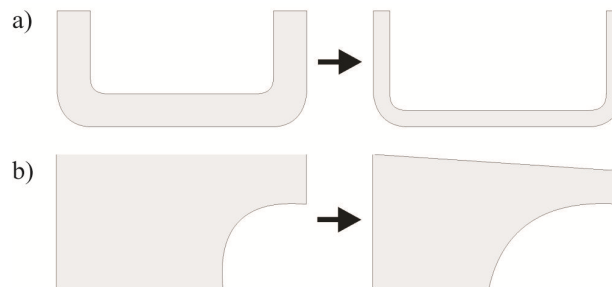


**Fig. 1** Types of optimization: a) parametric optimization, b) shape optimization

The parametric optimization performs changes only in the structural properties while the geometry stays the same [4, 5]. The shape optimization aims at changing the shape of the part until the best combination of geometry dimensions is reached [6, 7].

The aim of this paper is to show how the shape optimization of an axle guard of running gear elements of a Hccrrs 2x2 axle car-carrying wagon can significantly extend the life of the machine part subjected to dynamic loads.

## 2. Technical data of the axle guard of running gear elements of Hccrrs 2x2 axle car-carrying wagon

The running gear basically contains wheel sets, a carrying suspension spring and suspensions. Axle guards are an integral part of the wheel set of twin-axle wagons and their primary role is to protect a free passage of the wagon in the curve, i.e. they are used for longitudinal and transverse guiding of the wheel set.

The primary role of the axle guards is to receive longitudinal forces in the processes of braking and accelerating and transverse forces in curves (especially when travelling through the "S" curve). When passing through the curve the role of the axle guard is to allow the axis rotation of the wheel set in relation to the longitudinal axis of the wagon. The structure of the axle guard significantly affects the ride quality of the wagon.

According to the UIC 517 standard [8] there are three types of axle guards: ordinary axle guards with constant stiffness, reinforced axle guards with constant stiffness and axle guards with progressive stiffness. Axle guards for a wheel of a standard diameter of $\phi 920\,\text{mm}$ have standard carrying suspension springs and their characteristics are defined by the UIC 517 standard [8]. Wagons that have a smaller diameter of the wheel $\phi 630-840\,\text{mm}$ have an "explicit" construction of the axle guard which is in accordance with the diameter of the wheel and the wagon floor height. Basically, all types of axle guards, even those with a modified structure, need to comply with the requirements of the UIC 517 standard [8].

The considered axle guard of running gear elements of the Hccrrs 2x2 axle car-carrying wagon is a reinforced axle guard with constant stiffness (linear characteristics). It is exposed to low cycle fatigue and must meet requirements for static and fatigue loads according to the UIC 517 standard, point 3.1 and 3.2, Appendix L2 [8].

The carrying parts of the running gear elements of the Hccrrs 2x2 axle car-carrying wagon are made of the S355J0 steel grade, while the material of the axle guard is the S355J2+N steel. The mechanical characteristics of the S355J2+N steel in relation to nominal thicknesses according to the EN10025-2:2007 standard are shown in Table 1 [9].

**Table 1** Physical and mechanical characteristics of material (axle guard)

| Material (Steel mark) | Young Modulus $E$ / MPa | Density $\rho$ / kg/m$^3$ | Poisson ratio $\nu$ | Yield Strength $16 < \delta < 40$ $R_e$ / MPa | Tangent Modulus $E_T$ / MPa [10] |
|---|---|---|---|---|---|
| S355J2+N | $2.1 \cdot 10^5$ | $7.85 \cdot 10^{-6}$ | 0.3 | 345 | 2000 |

## 3. Fatigue material characterization

This section describes a fatigue characterization of the S355J2+N steel grade. The axle guard of the running gear elements of the Hccrrs 2x2 axle car-carrying wagon is made of the S355J2+N steel grade. Table 2 shows the results of the uniaxial tension–compression tests (loading ratio $R = -1$) of specimens made of the S355J2+N material [11].

**Table 2** Experimental tension–compression fatigue test results for S355J2+N material

| Number of specimens | $\varepsilon_a$ / % | $\sigma_a$ / MPa | Number of cycles $N_f$ |
|---|---|---|---|
| 1 | 0.20 | 281.18 | 64710 |
| 2 | 0.20 | 290.83 | 38685 |
| 3 | 0.20 | 279.41 | 94907 |
| 4 | 0.18 | 274.08 | 93974 |
| 5 | 0.18 | 273.18 | 161585 |
| 6 | 0.18 | 273.19 | 142942 |
| 7 | 0.17 | 276.48 | 274622 |
| 8 | 0.17 | 270.44 | 236083 |
| 9 | 0.17 | 270.09 | 192869 |
| 10 | 0.16 | 263.078 | 226521 |
| 11 | 0.16 | 257.68 | 374295 |
| 12 | 0.16 | 264.34 | 295734 |
| 13 | 0.15 | 254.18 | 426517 |
| 14 | 0.15 | 253.1 | 1212701 |
| 15 | 0.15 | 258.16 | 392807 |

In Table 2, $\varepsilon_a$ represents the range of strain amplitude and $\sigma_a$ represents the value of normal stress calculated by means of the maximal load applied to the cross-section $\left(\sigma_a = F/A_0\right)$. The uniaxial tension–compression tests were performed at five levels with a range of strain amplitude from 0.15 % to 20 % and with three repetitions per level.

Mathematical models used to describe the uniaxial tension–compression fatigue behaviour of the S355J2+N material, i.e. the $\varepsilon - N$ cyclic curve, are created by taking Ramberg–Osgood's approach [12], presented by equations (1-3)

$$\varepsilon_a = \varepsilon_{a,e} + \varepsilon_{a,p}, \tag{1}$$

$$\varepsilon_{a,e} = \frac{\sigma_a}{E}, \tag{2}$$

$$\varepsilon_{a,p} = \left(\frac{\sigma_a}{K'}\right)^{\frac{1}{n'}}, \tag{3}$$

and the approach presented by equation (4), which represents the sum of Basquin's and Manson-Coffin's part [12]

$$\varepsilon_a = \frac{\sigma'_f}{E} \cdot \left(2N_f\right)^b + \varepsilon'_f \cdot \left(2N_f\right)^c. \tag{4}$$

The mechanical parameters obtained from the uniaxial tension–compression fatigue tests of the S355J2+N material are shown in Table 3. The strain–life curve log–log representation is shown in Fig 2.

**Table 3** Mechanical properties of S355J2+N material under uniaxial cyclic tension–compression load

| Uniaxial cyclic tension–compression | Value |
|---|---|
| Strength coefficient $K'$ | 720.94 MPa |
| Strain hardening exponent $n'$ | 0,1258 |
| Cyclic yield strength $\sigma'_y$ | 330.0 MPa |
| Fatigue strength coefficient $\sigma'_f$ | 525.31 MPa |
| Fatigue strength exponent $b$ | -0.0521 |
| Fatigue ductility coefficient $\varepsilon'_f$ | 0.0662 |
| Fatigue ductility exponent $c$ | -0.3987 |
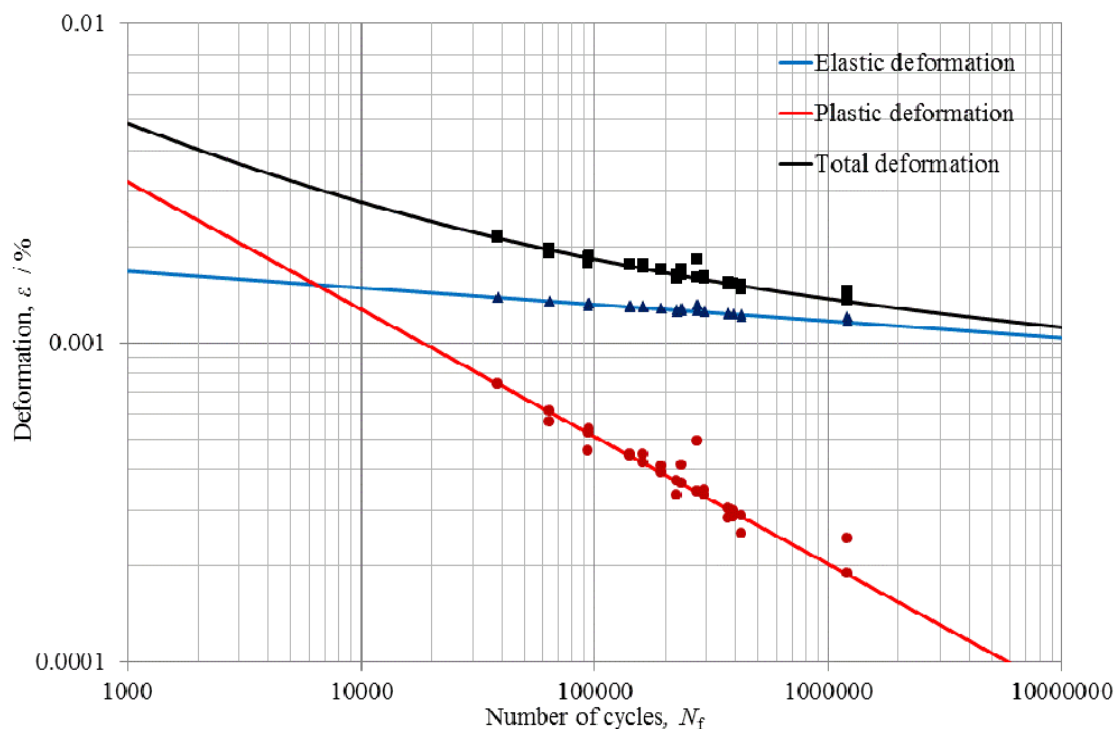


**Fig. 2** Strain–life curve resulting from uniaxial tension–compression fatigue tests of S355J2+N material

## 4.  Rigidity analysis of the axle guard when maximum lateral force is applied

The longitudinal strength of the axle guards is defined according to the UIC 517 standard, point 3.2 [8], and must be sufficient to withstand the longitudinal force of 50 kN in an unloaded state, that acts 70 mm over the center line of the wheel sets. The position and the shape of the axle guard must be such that the longitudinal force causes torsional stresses of insignificant values.

The lateral elastic strength of the axle guards is defined according to the UIC 517 standard, point 3.1 [8]. If the lateral force acts on the axle 70 mm above the center line of the wheel sets in an unloaded state, it causes the elastic displacement of the point of force application according to the diagram shown in Appendix L2 [8] (Fig 3).
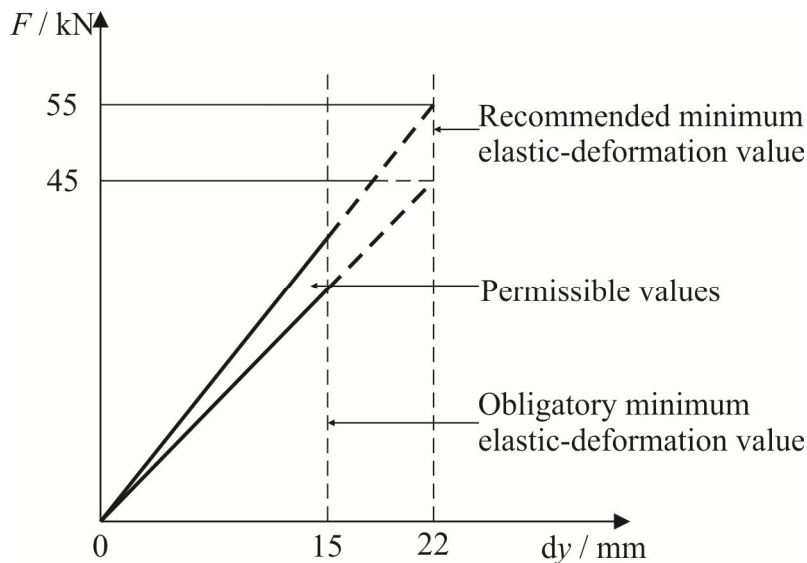


**Fig. 3**  Rigidity of axle guard with constant stiffness (reinforced type)

The most unfavorable load case in real conditions of exploitation was considered in the calculation of the ultimate fatigue strength of the axle guard. The most unfavorable load case is the case when the wagon is loaded with maximum payload and passes through the curve with the minimum radius. A scheme of the model loading in the case when the wagon passes through the curve with the minimum radius and when the maximum lateral force is applied on the axle guard is shown in Fig 4 [13].
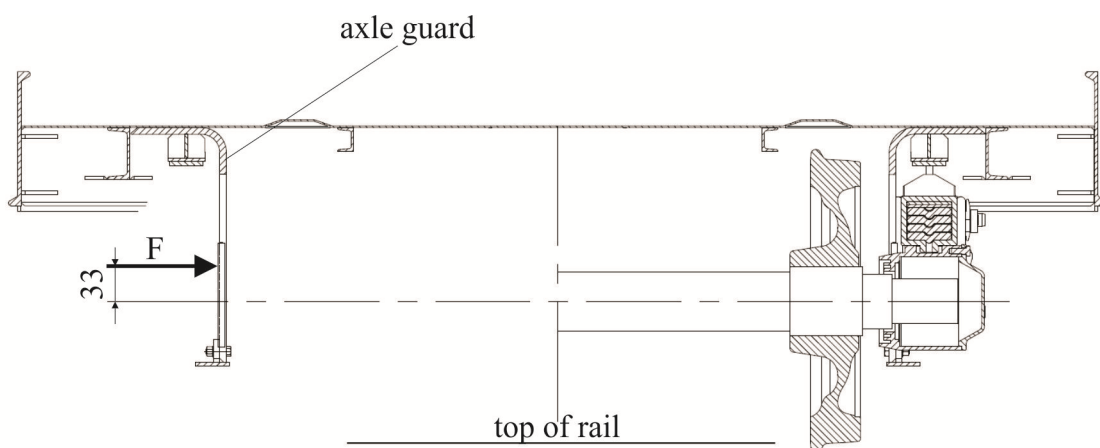


**Fig. 4**  Scheme of model loading; maximum lateral force for maximum stress of 345 MPa

## 4.1    Description of FEM model

The running gear elements of the Hccrrs 2x2 axle car-carrying wagon are modelled by using the Femap software with the NX Nastran solver [13], which is based on the finite element method. According to the design type, rectangular and triangular (four and three nodes, respectively) shell elements of appropriate thicknesses are used for creating a finite element mesh. The element length is approximately 40 mm. The 3D model of the running gear of the Hccrrs 2x2 axle car-carrying wagon with the old and the new optimized shape of the axle guard is shown in Fig 5 and Fig 6, respectively.
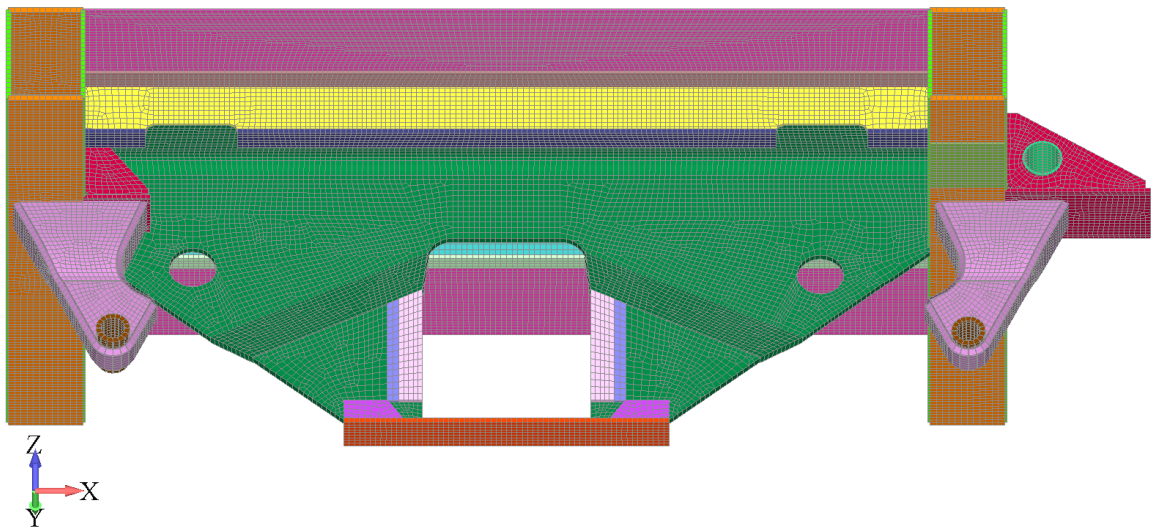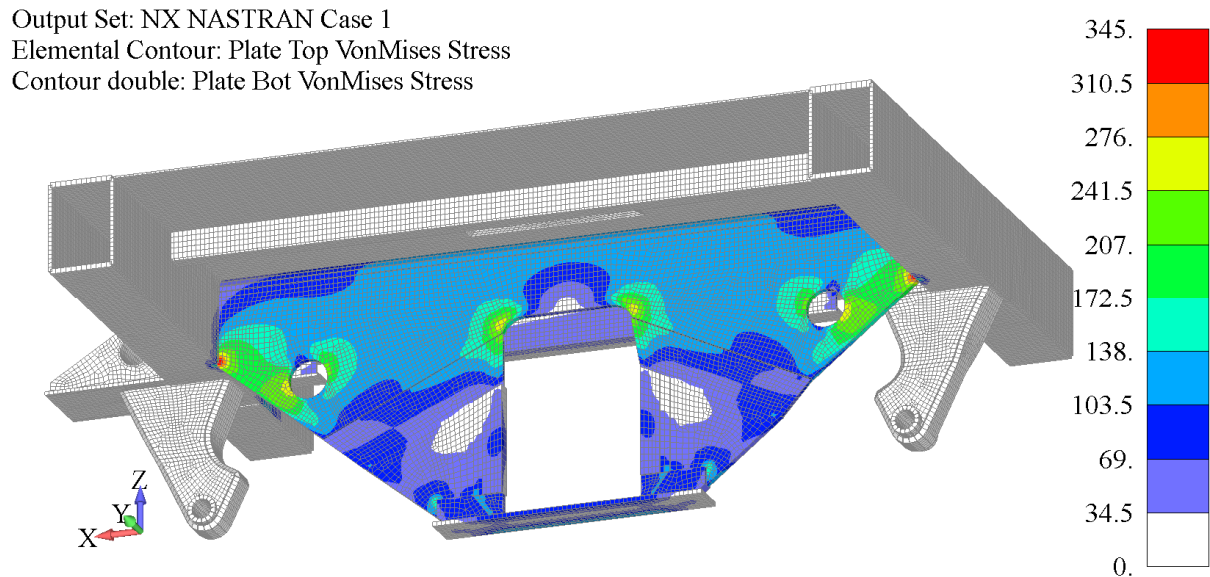


**Fig. 5** 3D model of running gear of Hccrrs 2x2 axle car-carrying wagon with old shape of axle guard – finite element mesh
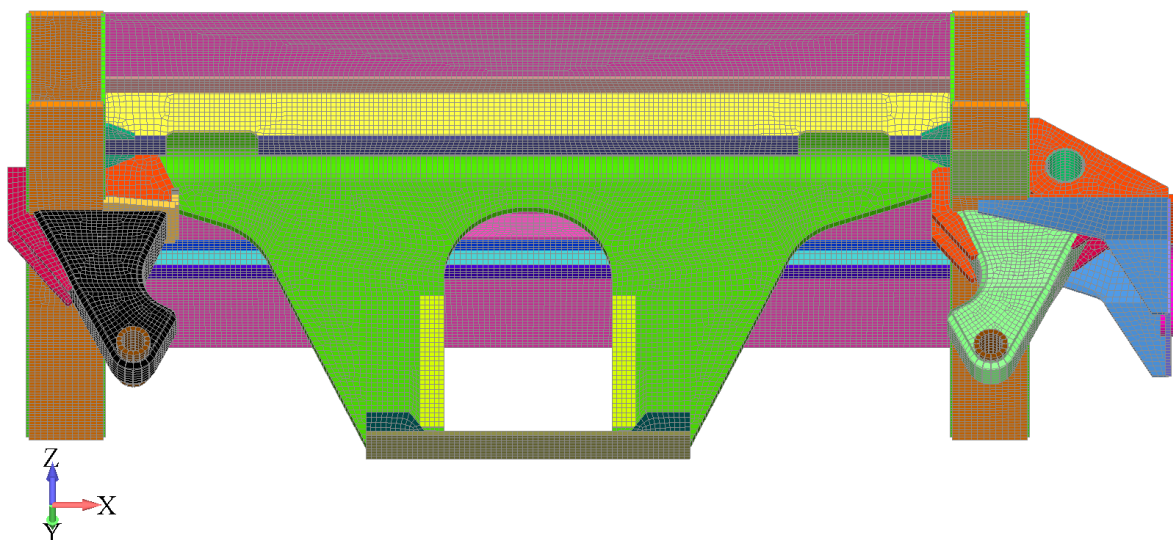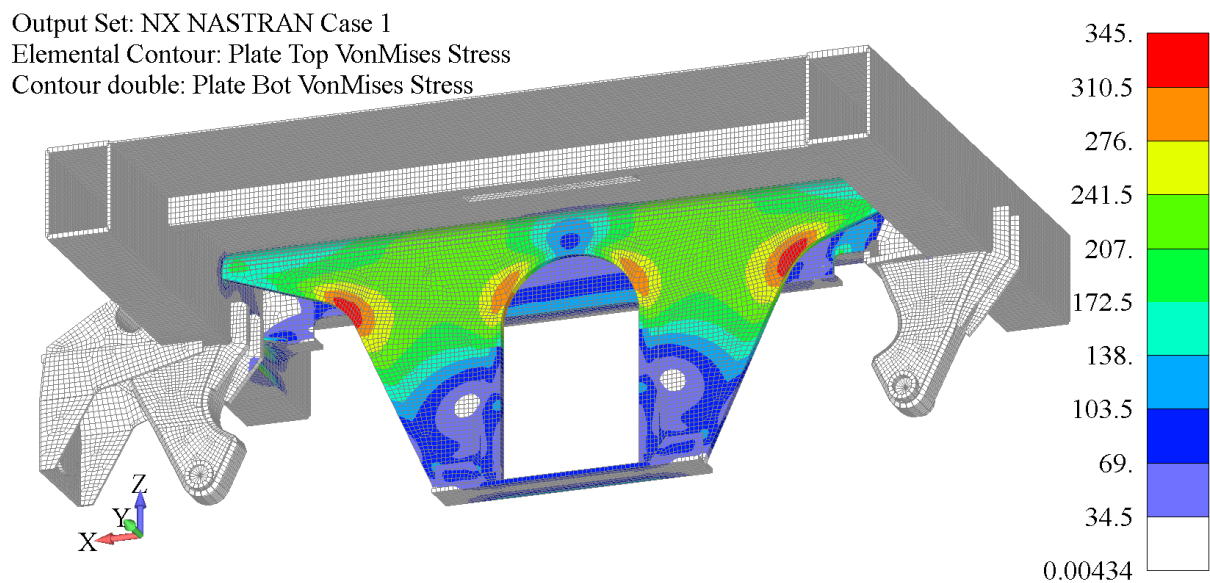


**Fig. 6** 3D model of running gear of Hccrrs 2x2 axle car-carrying wagon with new optimized shape of axle guard – finite element mesh

## 4.2   Calculation results

According to the scheme of the model loading shown in Fig. 4, the finite element analysis of rigidity was done for both shapes of the axle guards when the maximum lateral force is applied to the axle guard. The field of the von Mises equivalent stress on the models with the old and the new optimized axle guard is shown in Fig. 7 and Fig. 8, respectively. The displacement field in the lateral direction of the model with the old and the model with the new optimized shape of the axle guard is shown in Fig. 9 and Fig. 10, respectively.



Output Set: NX NASTRAN Case 1
Elemental Contour: Plate Top VonMises Stress
Contour double: Plate Bot VonMises Stress

**Fig. 7**  Von Mises equivalent stress field - model with old shape of axle guard



Output Set: NX NASTRAN Case 1
Elemental Contour: Plate Top VonMises Stress
Contour double: Plate Bot VonMises Stress

**Fig. 8**  Von Mises equivalent stress field - model with new optimized shape of axle guard

The maximum value of the von Mises equivalent stress for both shapes of the axle guards does not exceed 345 MPa. In order to achieve the maximum value of the von Mises equivalent stress, it is necessary to load both shapes of the axle guards with different values of

the maximum lateral force. In case of the old shape of the axle guard (Fig. 5), it is necessary to apply the maximum lateral force of 26.5 kN in order to obtain the maximum value of the von Mises equivalent stress of 345 MPa. In this load case, the lateral displacement of 11.15 mm is obtained at the point of application of the maximum lateral force.
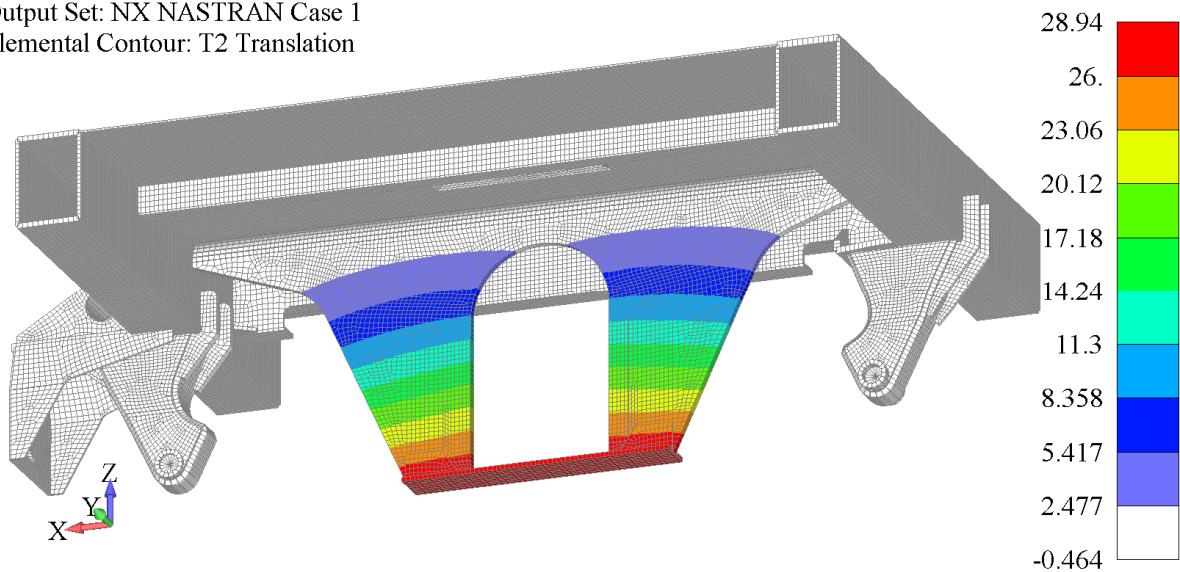
In the case of the new optimized shape of the axle guard (Fig. 6), it is necessary to apply the maximum lateral force of 38.4 kN in order to obtain the maximum value of the von Mises equivalent stress of 345 MPa. In this load case, the lateral displacement of 18.31 mm is obtained at the point of application of the maximum lateral force.
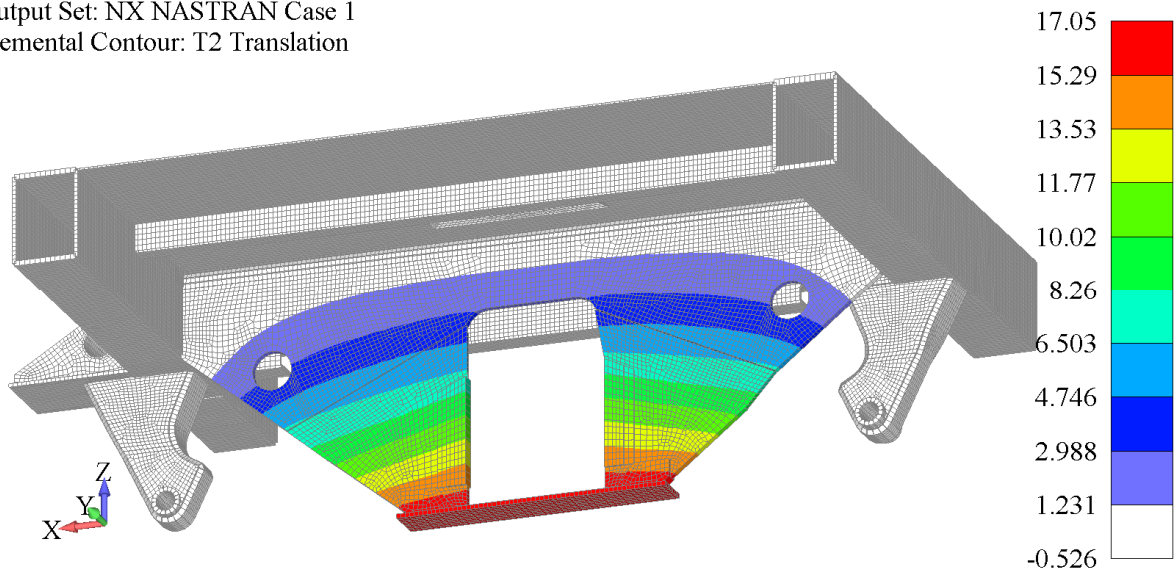


**Fig. 9** Lateral displacement field – $U_y$ – model with old shape of axle guard



**Fig. 10** Lateral displacement field – $U_y$ – model with new optimized shape of axle guard

If we compare the values of the forces that are necessary to achieve the maximum value of 345 MPa, it can be noticed that the old shape of the axle guard represents 74% of the

carrying of the new optimized shape of the axle guard. Also, if we compare the values of the lateral displacement at the point of application of the maximum lateral force, it can be noticed that the displacement of the old shape of the axle guard represents 61% of the displacement of the new optimized shape of the axle guard. However, according to the obtained values of the maximum forces and the corresponding displacements in the lateral direction, at the point of application of the maximum lateral force (diagram shown in Fig. 11), it can be seen that the intersection points of the corresponding maximum lateral forces and the corresponding lateral displacements are within the area of permissible values. The permissible values of the rigidity of the axle guard with constant stiffness (reinforced type) are defined according to the UIC 517 standard, Appendix L2 [8] and shown in Fig 3.
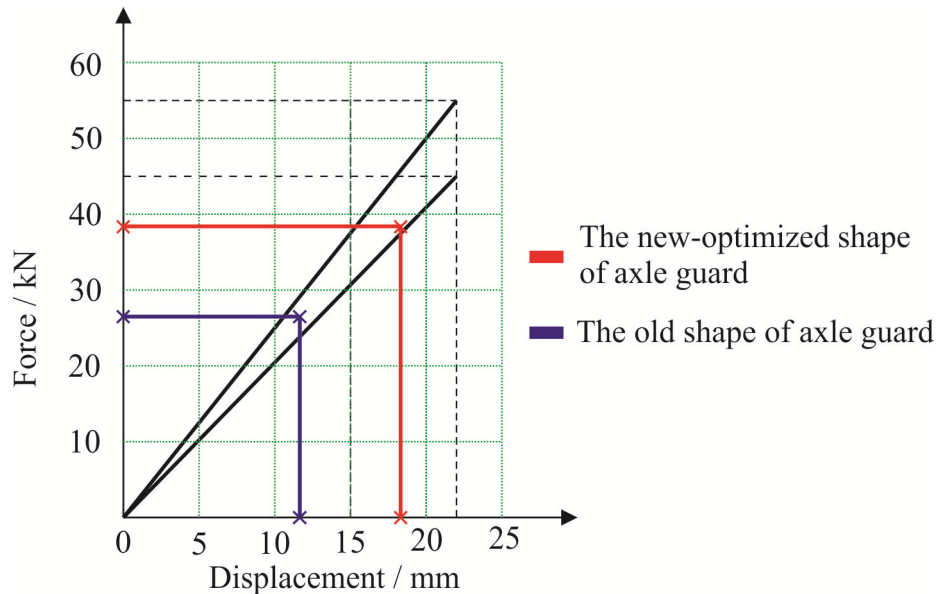


**Fig. 11**  Rigidity of axle guards at von Mises equivalent stress of 345 MPa

## 5. Elastoplastic analysis of axle guard in the case of lateral displacement of 22 mm

The aim of the elastoplastic analysis of the axle guard is the determination of the plastic strain field. Number of cycles before damage can be determined based on the maximum value of the plastic strain. A scheme of the model loading used for the elastoplastic analysis, in the case of the axle guard lateral displacement of 22 mm at the point of longitudinal force application, is shown in Fig 12.
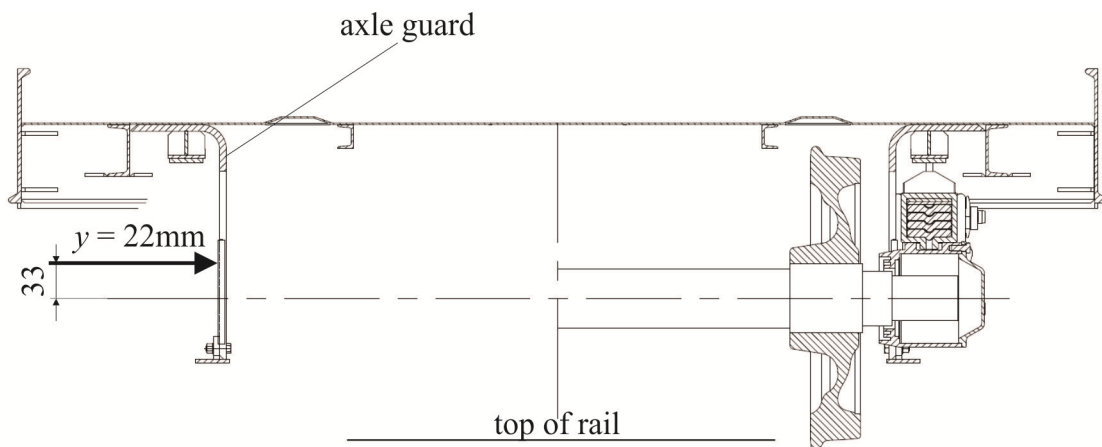


**Fig. 12**  Scheme of model loading; maximum lateral displacement $y = 22$ mm

The total strain fields calculated by using the elastoplastic analysis for the old and the new optimized shape of the axle guard are shown in Fig. 13 and Fig. 14, respectively. The plastic strain fields calculated by using the elastoplastic analysis for the old and the new optimized shape of the axle guard are shown in Fig. 15 and Fig. 16, respectively.
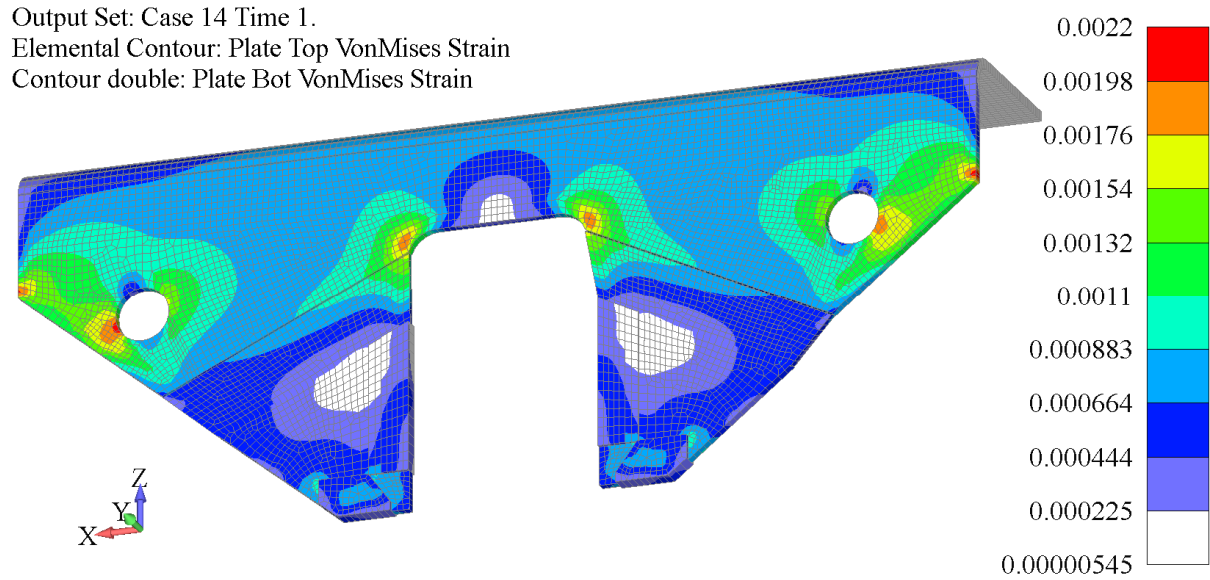


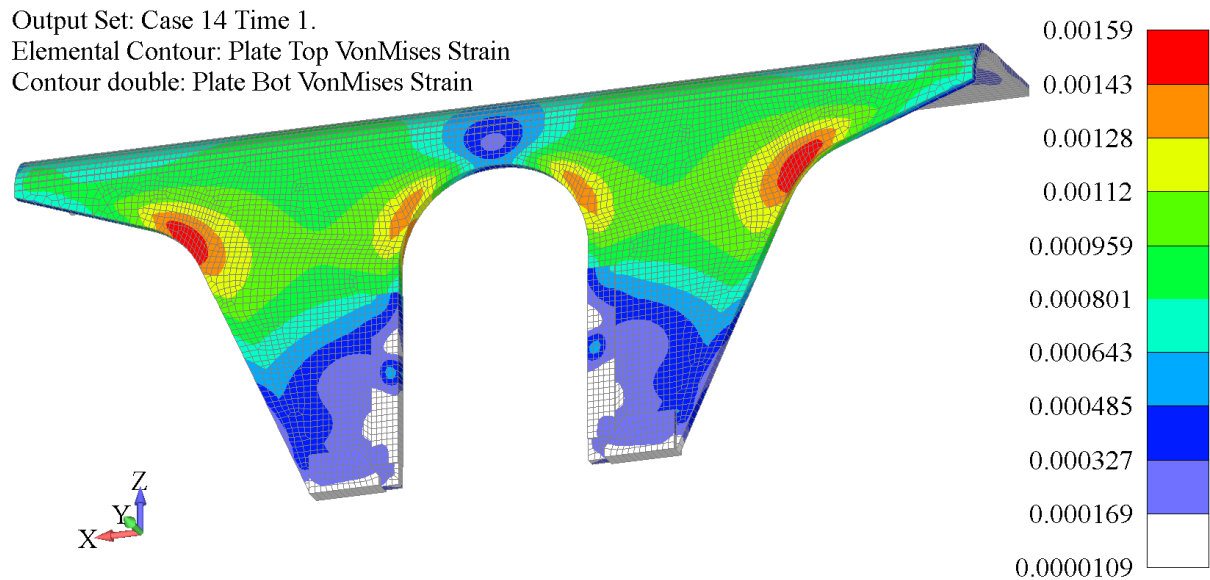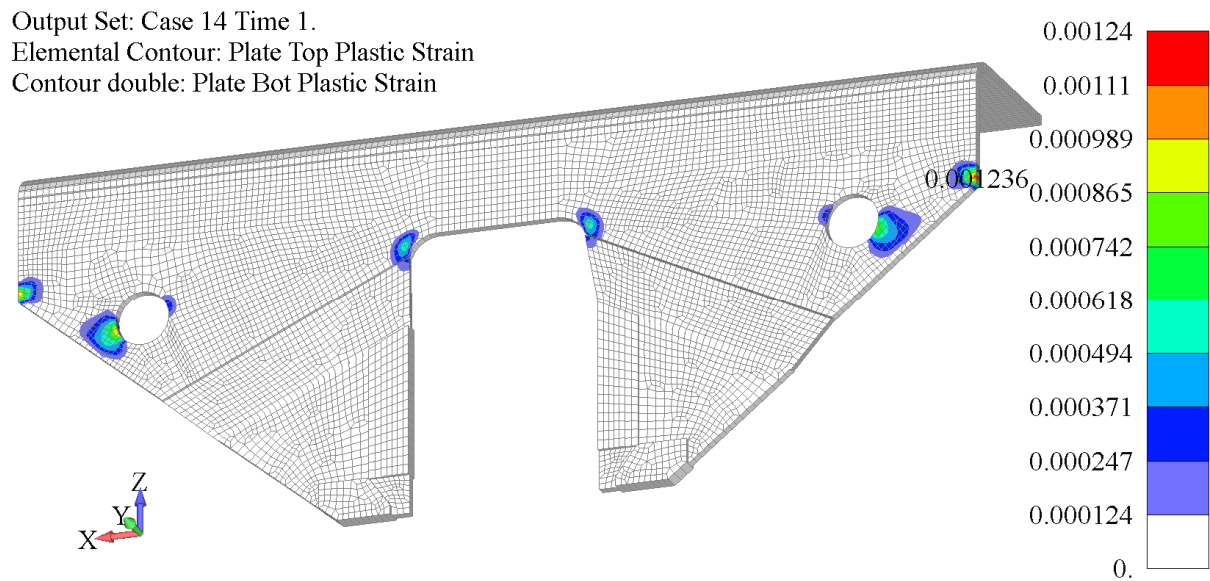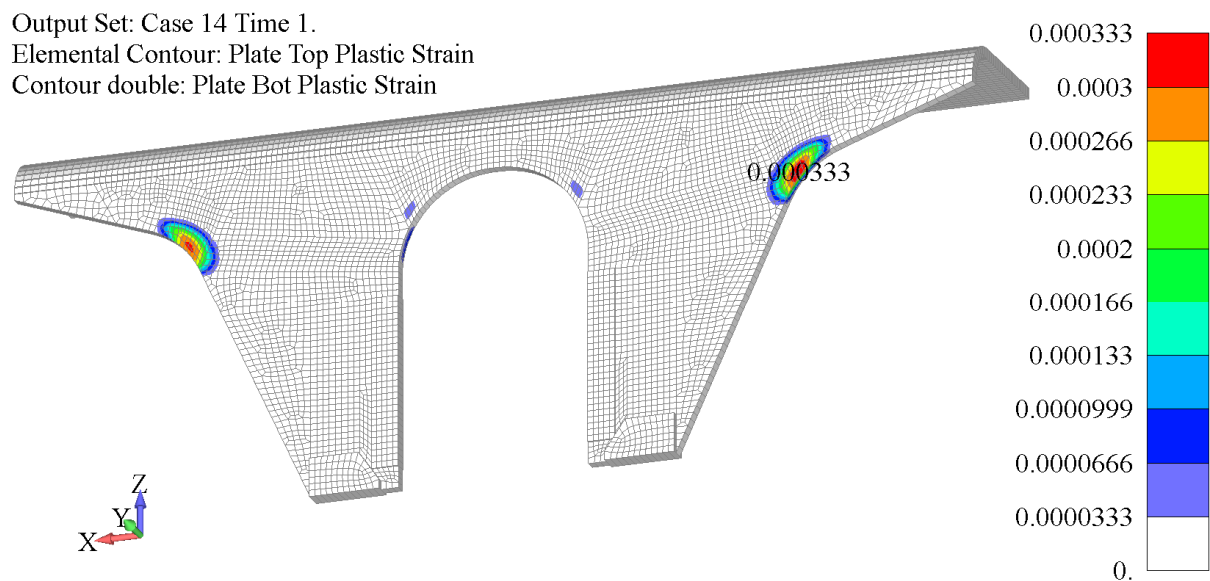**Fig. 13** Total strain field –old shape of axle guard



**Fig. 14** Total strain field –new optimized shape of axle guard

The maximum values of the plastic deformation of both shapes of the axle guards are shown in Fig. 15 and Fig. 16. The results of the elastoplastic analysis are required for the determination of the axle guard's fatigue strength, which is expressed with the number of cycles to failure. This means that the maximum value of the plastic deformation determines the number of cycles that the wagon structure part can withstand. The strain–life curve, determined experimentally for the S355J2+N steel grade, is shown in Fig. 17.

According to the results obtained by the FEM calculation, the maximum value of the plastic deformation of the old shape of the axle guard is 0.00124 (Fig. 15), while the maximum value of the plastic deformation of the new optimized shape of the axle guard is 0.000333 (Fig. 16).

Output Set: Case 14 Time 1.
Elemental Contour: Plate Top Plastic Strain
Contour double: Plate Bot Plastic Strain



**Fig. 15** Plastic strain field –old shape of axle guard

Output Set: Case 14 Time 1.
Elemental Contour: Plate Top Plastic Strain
Contour double: Plate Bot Plastic Strain



**Fig. 16** Plastic strain field –new optimized shape of axle guard

According to the values of the plastic deformation obtained for both shapes of the axle guards and the fatigue material properties of S355J2+N, the number of cycles to failure is determined. For the old shape of the axle guard, shown in Fig 5, the obtained fatigue life reaches 10673 cycles, while the obtained fatigue life of the new optimized shape of axle guard, shown in Fig 6, reaches 287937 cycles (Fig. 17). Based on the analysis of the obtained results it can be concluded that the shape optimization of the axle guard of the running gear elements of the Hccrrs 2x2 axle car-carrying wagon can significantly extend the fatigue life of the structure part subjected to dynamic loads.
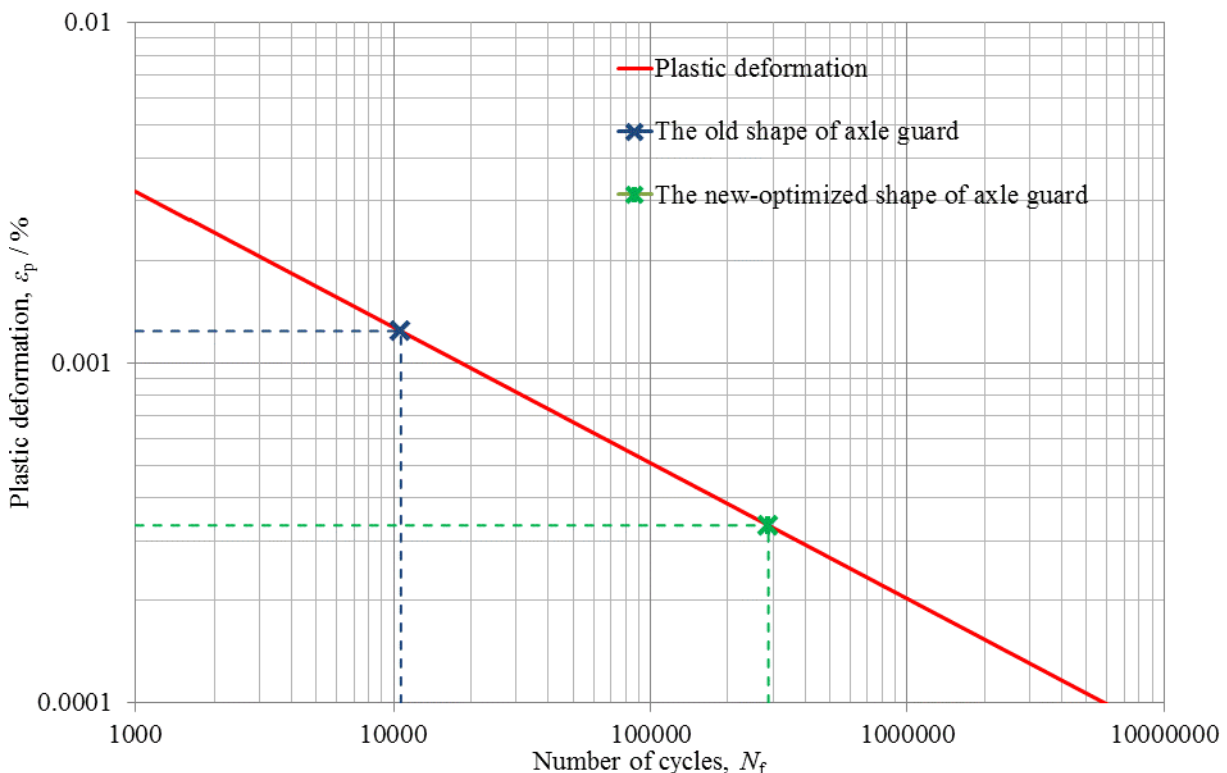


**Fig. 17** Plastic strain-life curve of S355J2+N material obtained by calculation of old and new optimized shape of axle guard

## 6. Conclusion

The paper presents the $\varepsilon - N$ approach or a fatigue analysis based on strain, which assumes that the critical areas of material behavior depend on the strain. The influence of shape optimization on the ultimate fatigue strength of the wagon structure part is shown on one practical example. The wagon structure part used for this study is the axle guard of running gear elements of the Hccrrs 2x2 axle car-carrying wagon exposed to a low cycle fatigue. The results of the FEM calculation (linear and elastoplastic) show higher stiffness and better fatigue properties of the new optimized shape of the axle guard. The number of cycles to failure is determined according to the maximum value of the plastic deformation and the obtained fatigue material properties of the axle guard. The results of the analysis show that the new optimized shape of the axle guard has a significantly longer fatigue life.

The methodology presented in this paper contains an experimental definition of fatigue parameters, shape optimization, a definition of the numerical model, numerical calculation of strength according to standards and estimation of fatigue strength by using experimental and

numerical results. The developed methodology based on the application of numerical, theoretical, and experimental techniques of fatigue mechanics has proven to be a powerful tool for the assessment of the fatigue life of structures exposed to dynamic loads.

## Acknowledgment

## REFERENCES

[1]   Hobbacher, A., editor, Recommendations for Fatigue Design of Welded Joints and Components, IIW Document XIII-1823-07, update 2008.

[2]   Lassen T., Recho N., *Fatigue Life Analysis of Welded Structures*, ISTE Ltd, 2006

[3]   F. Berto, P. Lazzarin, *Fatigue strength of structural components under multi-axial loading in terms of local energy density averaged on a control volume,* International Journal of Fatigue, Volume 33, pp. 1055-1065, (2011)

[4]   S. Hertelé, W. De Waele, R. Denys, M. Verstraete, J. Van Wittenberghe, *Parametric finite element model for large scale tension tests on flawed pipeline girth welds*, Advances in Engineering Software, Volume 47, Issue 1, pp. 24–34, (2012)

[5]   Marko Topalović, Vladimir Milovanović, Milan Blagojević, Aleksandar Dišić, Dragan Rakić, Miroslav Živković, *Freight Wagon Mass Reduction using Parametric Optimisation*, VIII Triennial International Conference „Heavy Machinery-HM 2014", Zlatibor, Serbia, 2014, 25-28 June, pp E.53-60, ISBN 978-86-82631-74-3

[6]   M. Firl, R. Wüchner, K. U. Bletzinger, *Regularization of shape optimization problems using FE-based parametrization*, Structural and Multidisciplinary Optimization, Volume 47, Issue 4, pp. 507-521, (2013)

[7]   B. Hassani, S. M. Tavakkoli, H. Ghasemnejad, *Simultaneous shape and topology optimization of shell structures*, Structural and Multidisciplinary Optimization, Volume 48, Issue 1, pp. 221-233, (2013)

[8]   *International Standard UIC Code 517: Wagons - Suspension gear - Standardisation 7th edition,* May 2007

[9]   *EN 10025-2:2007 European Standard Structural Steel,* 2007.

[10]  K. D. Tsavdaridis and C. D'Mello, *Optimisation of Novel Elliptically-Based Web Opening Shapes of Perforated Steel Beams*, Journal of Constructional Steel Research*,* Volume 76, pp. 39-53, 2012.

[11]  C. Gomez, M. Canales, S. Calvo, R. Rivera, J. R. Valdes and J. L. Nunez, *High and Low Cycle Fatigue Life Estimation of Welding Steel Under Constant Amplitude Loading: Analysis od Different Multiaxial Damage Models and In-Phase and Out-phase Loading Efects*, International Journal of Fatigue*,* Volume 33, pp. 578-587, 2011.

[12]  R. Stephens, A. Fatemi, R. Stephens and H. Fuchs, *Metal Fatigue in Engineering*, New York: John Wiley & Sons Inc., 2001.

[13]  *FEMAP, version 10 user guide. Munich, Germany: Siemens Product Lifecycle Management Software Inc.,* 2009.

Submitted:        09.6.2015             Vladimir Milovanović, PhD student
                                        Miroslav Živković, PhD
Accepted:         14.10.2015            Gordana Jovičić, PhD
                                        Jelena Živković, PhD student
                                        Faculty of Engineering, University of Kragujevac
                                        Dražan Kozak, PhD
                                        Mechanical Engineering Faculty
                                        Slavonski Brod, Josip Juraj Strossmayer University of Osijek